

Lanthanide Supramolecular Transformers Induced by  $K^+$  and  $CO_2$ Bei Wang,<sup>\*,†</sup> Bing Ma,<sup>†</sup> Zhangwen Wei, Huan Yang, Meng Wang, Wenxia Yin, Hong Gao, and Weisheng Liu<sup>\*</sup>Cite This: *Inorg. Chem.* 2021, 60, 2764–2770

Read Online

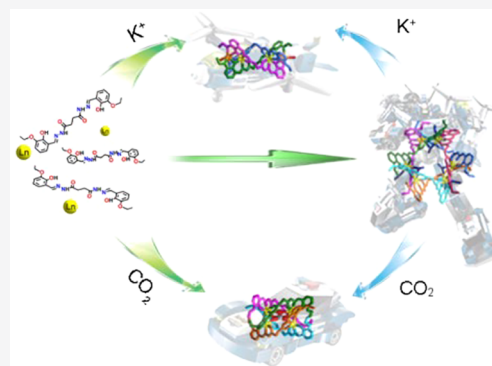
ACCESS |

Metrics &amp; More

Article Recommendations

Supporting Information

**ABSTRACT:** The transfer of configuration information from supramolecular helices is a ubiquitous phenomenon in nature. DNA and proteins often change their helical structure in response to particular external stimuli and can activate important related events through sophisticated mechanisms. Attempts to create artificial multiple-stranded helicates that can adjust the configuration under external stimuli have also met with limited success. Using a simple ligand, we now show multiple-stranded lanthanide helicates that transform efficiently. Lanthanide and ligand are successfully self-assembled into different multiple helical supermolecular clusters using different templates. Additionally, these intelligent supermolecular transformers can also be transformed by different external stimuli and realize the selective recognition and fixation of the corresponding ions and molecules.



## INTRODUCTION

Research into supramolecular chemistry has intensified significantly during the last 2 decades, with a focus on the design of multicomponent assemblies with more sophisticated functionalities.<sup>1</sup> Multiple-stranded helicates are of interest because of their geometric simplicity and significance in biology and materials. Self-assembled lanthanide supramolecular systems, especially multiple-metallic helicates, have attracted increasing attention because of their magnetic and spectroscopic properties.<sup>2</sup> However, the control and precise prediction of stereoselective results is still a great challenge during lanthanide supramolecular assemblies.<sup>3</sup> Because lanthanide ions are known to have variable coordination numbers, kinetic lability, and poor stereochemical preferences, the precise prediction and control of the resulting stereoselectivity of lanthanide supramolecular assemblies remains an important and challenging issue.

The transfer of configuration information from supramolecular helices is a ubiquitous phenomenon in nature. DNA and proteins often change their helical structure in response to particular external stimuli and can activate important related events through sophisticated mechanisms.<sup>4</sup>

Potassium ions play a crucial role in numerous biological processes, including maintenance of fluid and electrolyte balances in the body, thus making their selective detection rather important for biomedical diagnosis and environmental remediation.<sup>5</sup> Although a number of potassium(I) probes have been proposed,<sup>6</sup> lanthanide multiple helicates exhibiting high selectivity and affinity for potassium have not been extensively developed.<sup>7</sup> On the basis of the results of previous studies, we hypothesized that by careful design of the ligands and choice of the metal ions, the optimum coordination environment for

special alkaline or alkaline-earth ions might be obtained inside an easily assembled supramolecular structure. To test this, we constructed lanthanide helicate clusters designed to selectively recognize  $K^+$  rather than classic receptors comprised of crown or lariat ethers.<sup>8</sup>

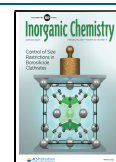
Additionally, the fixation and activation of atmospheric carbon dioxide ( $CO_2$ ) is an area of immense research interest to the scientific community.<sup>9</sup> The effective conversion of  $CO_2$  to useful chemicals is frequently achieved using transition-metal-based chemistry and catalysis<sup>10</sup> but rarely with lanthanide helicates.<sup>11</sup> We designed this ligand to be able to capture  $CO_2$  to form lanthanide multiple helicates, and the helicates can be configured in a variety of configurations because of different environments, just like transformers.

Previously, we reported the first example of lanthanide multiple helicates altering their helical configurations in the presence of nitrate ions.<sup>12</sup> In this paper, we report efforts to predict and control the configuration changes of new lanthanide multiple helicates by selective recognition toward  $K^+$  or  $CO_2$ .

The linear bis(acylhydrazone) ligand  $H_2L$  is versatile, and the self-assembly process depends strongly on templates. Thus, in the presence of the larger tetrahedral anion  $ClO_4^-$ , the larger circular helicate is favored,<sup>12</sup> whereas  $K^+$  and atmospheric  $CO_2$

Received: December 12, 2020

Published: February 1, 2021

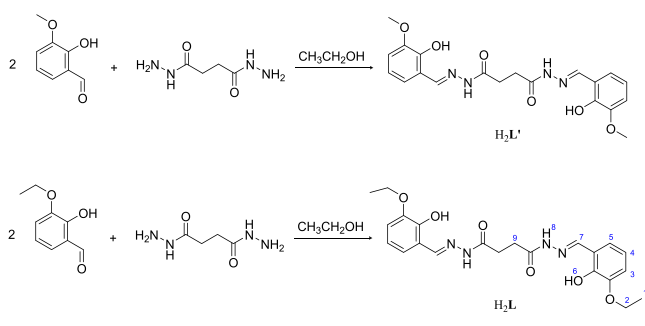


induce the formation of *s*–*f* tetranuclear dimetallic triple-stranded helicates and tetranuclear quadruple-stranded lanthanide helicates, respectively. More interestingly, the  $K^+$  and  $CO_2$  templates successfully induced the circular helicates to transform into either an *s*–*f* heterotetrametallic triple-stranded helicate or a tetranuclear quadruple-stranded lanthanide helicate, respectively, just like the intelligent molecular transformers, which can be assembled into different configurations under different conditions, and can be reconstructed under different external stimuli.

## RESULTS AND DISCUSSION

**$K^+$ -Induced Lanthanide Helicate Supramolecule Identification Self-Assembly.** A linear tetradentate ligand  $H_2L'$ , is comprised of two binding strands anchored to a flexible spacer (Scheme 1). This structure adopts a linear con-

Scheme 1. Syntheses of  $H_2L'$  and  $H_2L$



formation favoring a dinuclear triple-stranded helicate (complex 3, Figure 1a). Structural analysis of complex 3 revealed that the two holes at both ends of the helicate are formed by six oxygen atoms, respectively. This helicate possesses internal oxygen-donor atoms, and therefore templat-

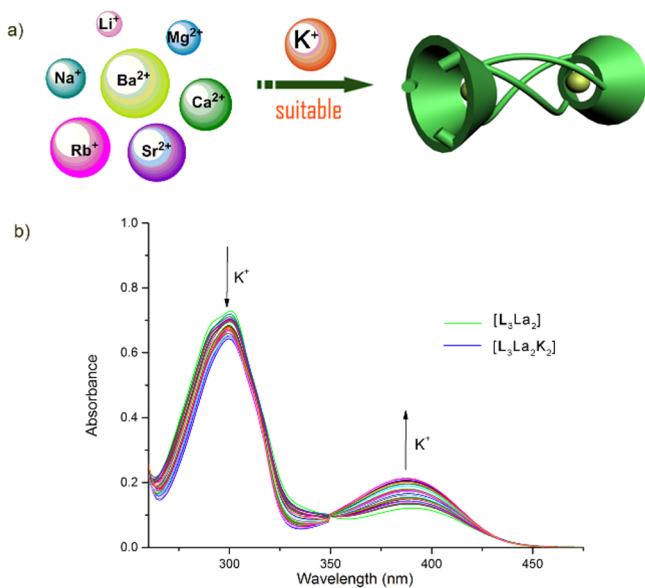


**Figure 1.** (a) Schematic representation of the lanthanide helicate clusters for the recognition and fixation of  $K^+$ . (b) UV–vis spectral changes for the compound  $[L_3La_2]$  with  $K^+$  (0–4.0 equiv) in acetonitrile.  $[L_3La_2] = 0.67 \times 10^{-5}$  M;  $[K^+] = 0, 0.02, 0.04, 0.06, 0.08, 0.10, 0.12, 0.14, 0.16, 0.18, 0.2, 0.4, 0.6, 0.8, 1.0, 1.2, 1.4, 1.6, 1.8, 2.0, 3.0,$  and 4.0 equiv.

ing by cations is possible. This templating depends on the “size selectivity” between the template and the cavity of the helicate (“lock-and-key principle”). Interestingly, for each cavity, the distance from the center to the six ligand oxygen atoms is about 3.0 Å, which is equal to the coordinate bond length of  $K$ –O.<sup>7</sup> Consequently, the cavity exhibits high selectivity and affinity for potassium ions (Figure 1a).

Complex 3 was prepared from ligand  $H_2L'$  and cerium chloride in a 1:1 ratio (Figure 2a), whereas compounds 4a and 4b were obtained from the ligand  $H_2L$ , KOH, and lanthanide halide salts (1:2:1). KOH was added as a base and a template (Figure 2b). As anticipated, 4a and 4b both captured and fixed  $K^+$  effectively (Figures S6 and S8). X-ray crystallographic studies revealed that the crystals 4a and 4b have isostructural relationships and belong to the monoclinic space group  $P2_1/c$ . To the best of our knowledge, complexes 4a and 4b are the first examples of *s*–*f* tetranuclear dimetallic helicates.

The skeletal structure of complex 4a consists of two  $La^{3+}$  ions, two  $K^+$  ions, three deprotonated ligands, and two coordinated water molecules, forming  $[K_2La_2L_3(H_2O)_2]^{2+}$ . Additionally, two  $Br^-$  counteranions are observed in the complex (Figure S6). The three ligand strands wrap around the four metals and form the conformation of a tetranuclear dimetallic triple-stranded helicate. The metal ions are approximately aligned [ $\angle K1 \cdots La1 \cdots La2, 167.250(4)^\circ$ ;  $\angle La2 \cdots La1 \cdots K1, 176.270(4)^\circ$ ], both  $K1 \cdots La1$  and  $K2 \cdots La2$  are regularly spaced by approximately 3.77 Å [ $K1 \cdots La1, 3.7345(14)$  Å;  $K2 \cdots La2, 3.8027(15)$  Å], and the  $La1 \cdots La2$  distance is 7.1150(6) Å. Each  $K^+$  ion is coordinated by seven coordination atoms, with three phenolic hydroxy and ethoxy units from three different ligands and one solvent  $H_2O$  molecule in a disordered monocapped three-prism arrangement (Figure S7). In addition, each  $La^{3+}$  ion is coordinated by nine coordination atoms, arising from the coordination of three tridentate salicylaldehyde–hydrazone domains from three different ligands ( $La$ –N, 2.729–2.808 Å;  $La$ –O, 2.381–2.613 Å), consequently three nitrogen atoms together with six oxygen atoms establish the coordination geometry of  $La^{3+}$ , which can be best described as a distorted monocapped square antiprism. Confirmation of the roles of  $K^+$  ions in the self-assembly process is demonstrated by its inability to form analogous helicate structures with other alkali- and alkaline-earth-metal ions. As designed, the restricted geometric constraints of the cavities provide high selectivity of the helical recognizers toward  $K^+$  ions over other ions such as  $Li^+$ ,  $Na^+$ ,  $Rb^+$ ,  $Mg^{2+}$ ,  $Ca^{2+}$ ,  $Sr^{2+}$ , and  $Ba^{2+}$ .

Additional experiments under identical conditions were conducted to further investigate the ability of these lanthanide-based helical complexes to selectively bind  $K^+$  over other alkaline and alkaline-earth metals. These methods included UV–vis absorption, high-resolution electrospray ionization mass spectrometry (HR-ESI-MS), and  $^1H$  NMR.

The UV–vis absorption spectrum of compound  $[L_3La_2]$  was recorded in an acetonitrile solution. Upon the addition of 0–4.0 equiv of  $K^+$  to the compound, the absorbance at 301 nm slightly decreased while the absorption at 390 nm gradually increased, suggesting the coordination of  $K^+$  with this compound (Figures 1b and S13). Absorption titrations of this compound with various alkaline and alkaline-earth ions were conducted to examine the selectivity (Figure S14). Changes in the spectra were not observed in the presence of other cations such as  $Li^+$ ,  $Na^+$ ,  $Rb^+$ ,  $Mg^{2+}$ ,  $Ca^{2+}$ ,  $Sr^{2+}$ , or  $Ba^{2+}$ , indicating selective recognition in the presence of  $K^+$ . The

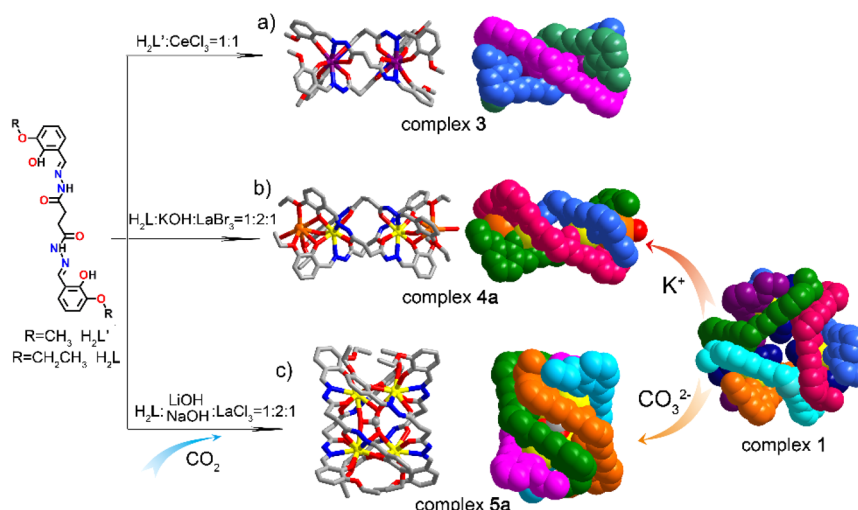


**Figure 2.** Self-assembly of helicates **3**, **4a**, and **5a** from ligands and the transformations between the configurations (Ce, purple; La, yellow; K, orange; N, blue; O, red; C, gray). The ligands are represented in different colors. Hydrogen atoms, external counteranions, and solvent molecules are hidden for clarity.

selectivity of the helicate toward  $K^+$  was evidenced by detection of the corresponding HR-ESI-MS as well. Upon the addition of 2 equiv of different alkaline and alkaline-earth ions in the solution of compound  $[L_3Nd_2]$ , the main peak was observed at  $m/z$  875.15686, which represented complex  $[L_3Nd_2K_2(CH_3OH)_2]^{2+}$ , for  $K^+$  (Figure S15). The high selectivity of lanthanide complexes toward  $K^+$  among other alkali- and alkaline-earth-metal ions was attributed to the cavity size, geometry, and ligand distance of the oxygen atoms at the two termini of the helical structures.

The  $Nd^{3+}$  ion can be identified specifically because of its sharp emission band centered at 1060 nm. It is used in many potential applications including energy conversion, night vision, sensing, tracking, anticounterfeit printing, optical communication, and many other fields as the representative of near-IR (NIR) materials. Complex  $[L_3Nd_2]$  exhibited a strong unique emission of the  $Nd^{3+}$  ion at 1025–1125 nm, which can be assigned to the  ${}^4F_{3/2} \rightarrow {}^4I_{9/2}$  transition, pointing toward efficient sensitization of the  $Nd^{3+}$  ion. More importantly, the luminescent intensity of  $Nd^{3+}$  at 1058 nm increased rapidly with the addition of 0–2.0 equiv of  $K^+$  (Figure S16), exhibiting an obvious NIR luminescent response to  $K^+$ .

**Reconfiguration of Intelligent Molecular Transformers Induced by  $K^+$ .** To better understand the interactions between  $K^+$  and the lanthanide-based high-nuclearity clusters, we performed  $K^+$ -ion-templated self-assembly with hexanuclear lanthanide cyclic helicate  $[La_6L_6(CH_3O)_3(CH_3OH)_3](ClO_4)_3$  (**1**).<sup>12</sup> Composition changes based on the presence of  $K^+$  ions were confirmed by X-ray diffraction, IR, and  ${}^1H$  NMR studies. The addition of KI to a solution of **1** led to the crystallization of  $[K_2La_2L_3(H_2O)_2]^{2+}$ , which was confirmed by X-ray diffraction analysis, and did not lead to the formation of additional species, which suggests that the  $s$ - $f$  tetranuclear dimetallic helicate is the only thermodynamically favored assembly in solution. The IR spectra of  $H_2L$ , **4a**, **4b**, **1**, and **1** +  $K^+$  are presented in Figure S9. The IR spectrum of **1** +  $K^+$  is completely consistent with that of **4** but significantly different from that of **1**, which means that when we added  $K^+$  to **1**, the complex was completely converted to **4**. The  ${}^1H$  NMR spectrum of a methanol solution of  $[K_2La_2L_3(H_2O)_2]Br_2$

revealed the presence of one major set of 20 signals, assigned to the protons from three ligands (Figures 3e and S12). The

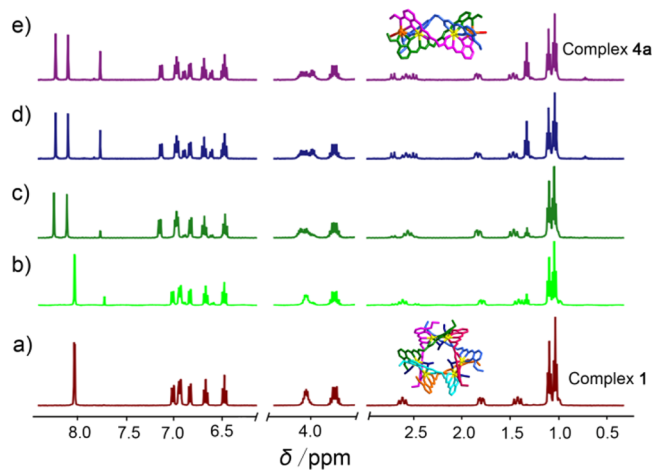


**Figure 3.**  ${}^1H$  NMR (400 MHz) titration of **1** (1.26 mM) with KI in  $CD_3OD$  by the addition of  $K^+/La^{3+}$  at different ratios (bottom to top): (b) 0.5; (c) 1.0; (d) 2.0, at 298 K for 4 days.

addition of KI to the 1.26 mM solution of **1** ( $K^+/La^{3+}$  1:2–2:1) in  $CD_3OD$  resulted in the progressive disappearance of the NMR signals belonging to **1** and the appearance of the signals assigned to **4a** (Figure 3), indicating that **1** changed into **4a** when induced by the  $K^+$  template.

Furthermore, when a mixture of all alkali- and alkaline-earth-metal chlorides was added to a methanol solution of complex **1**, chemical shift changes of the  ${}^1H$  NMR spectrum were consistent with the chemical shift changes of adding  $K^+$  only, which means that only  $K^+$  caused the configuration transformation, while other alkali metals and alkaline-earth metals had no influence. Diffusion-ordered NMR spectroscopy indicated a single product with a single band at the diffusion coefficient  $D = 7.827 \times 10^{-10} m^2 s^{-1}$  ( $\log D = -9.106$ ; Figure S17). Analysis of the  ${}^1H/{}^1H$  COSY NMR spectrum of the product also indicated results consistent with the spectrum of complex **4a**. These data indicated high selectivity and strong

specificity of the complex with  $K^+$  in a methanol solution over other alkali- and alkaline-earth-metal ions.

**CO<sub>2</sub>-Induced Lanthanide Helicate Supermolecule Identification Self-Assembly.** During the preparation of complex **4**, we found another interesting phenomenon. For the same synthesis conditions, just because of the absence of  $K^+$ , we got a completely different complex, **5**, which can capture and fix atmospheric CO<sub>2</sub> (Figure 2c). The fixation and activation of CO<sub>2</sub> in the atmosphere are becoming an important research field. The effective conversion of CO<sub>2</sub> to other useful chemicals is frequently achieved by using catalysts based on transition metals but rarely with lanthanide helicates.

X-ray crystallographic studies revealed that both crystals **5a** and **5b** belong to the triclinic space group  $P\bar{1}$ . The asymmetric unit is very similar to  $[La_4L_4(NO_3)](NO_3)_3$  (**2**), as previously reported.<sup>12</sup> Four Ln<sup>3+</sup> ions form a twisted rectangle, and four deprotonated ligands wrap around four Ln<sup>3+</sup> ions in a helical fashion, resulting in the formation of a tetranuclear quadruple-stranded helicate structure. The most notable structural feature of **5a** and **5b** is the encapsulated, distorted CO<sub>3</sub><sup>2-</sup> anion at the center in the cage, where the anion uses three oxygen atoms coordinated to four inner lanthanum ions in  $\mu_4-\eta^2:\eta^2:\eta^2$  and  $\mu_4-\eta^1:\eta^1:\eta^2$  bridging modes, respectively (Figures S18 and S20). From another viewpoint, the Ln<sup>3+</sup> ions are in close contact, and the supramolecular structure is further stabilized after the introduction of CO<sub>3</sub><sup>2-</sup>. The Nd<sup>3+</sup> complex **5b** displays efficient NIR emission upon excitation at 420 nm, arising from the <sup>4</sup>F<sub>3/2</sub> → <sup>4</sup>I<sub>J</sub> ( $J = 9/2, 11/2, 13/2$ ) transition (Figure S24). The NIR quantum yield of **5b** was  $1.43 \pm 0.10\%$ , and the luminescence lifetime was 0.21 μs (Table S1).

The reactions between the complexes and CO<sub>2</sub> were further investigated through IR and NMR spectroscopy. The IR spectra of the ligand and crystals (**5a** and **5b**) were measured in the solid state (Figure 4a). Carbonate-based vibrations, which cannot be observed from the ligand, are shown in the IR spectra of **5a** and **5b** at approximately 1500 cm<sup>-1</sup>. The presence of CO<sub>3</sub><sup>2-</sup> in **5a** was further confirmed by the results of solid-state <sup>13</sup>C NMR detection (Figure S26), which exhibited a low-intensity single peak at  $\delta = 172.40$  ppm that should be assigned to the encapsulated CO<sub>3</sub><sup>2-</sup>.<sup>11a,13</sup> To determine the origin of CO<sub>3</sub><sup>2-</sup> in the clusters, the same reactions of L<sup>2+</sup> with LaCl<sub>3</sub>·7H<sub>2</sub>O were carried out in methanol under an inert atmosphere (Ar or N<sub>2</sub>). When CO<sub>2</sub> was slowly bubbled into the solution, obvious changes in the UV absorption spectrum were observed. During the experiment, we observed that microcrystalline precipitation gradually appeared in solution with the introduction of CO<sub>2</sub> (Figure S27). We collected microcrystals for X-ray diffraction and IR, which confirmed that the composition was indeed that of complex **5a**. All of these results show that the CO<sub>2</sub> molecules are efficiently captured and fixed by these clusters through chemical conversion.

**Reconfiguration of Intelligent Molecular Transformers Induced by CO<sub>2</sub>.** It is interesting to note that CO<sub>2</sub> can also induce configuration transformation. When CO<sub>2</sub> was added to the solution of hexanuclear circular helicate **1**,<sup>12</sup> the quadruple-stranded helicate **5a** was crystallized and confirmed by X-ray diffraction analysis, thus indicating that **1** had changed into **5a** when induced by the CO<sub>2</sub> template. The IR spectra of H<sub>2</sub>L, **5a**, **5b**, **1**, and **1** + CO<sub>2</sub> are presented in Figure 4a. New carbonate-based vibrations at approximately 1500 cm<sup>-1</sup> can be observed from **5a**, **5b**, and **1** + CO<sub>2</sub>, which are different from **1** and the ligand.<sup>14</sup> Additionally, the HR-ESI-MS

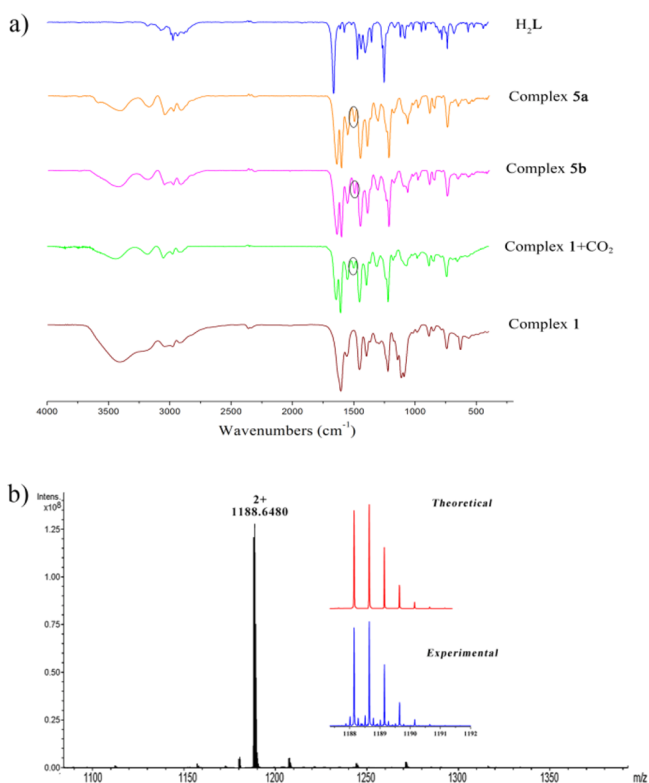


**Figure 4.** (a) IR spectra of ligand H<sub>2</sub>L and complexes (**5a**, **5b**, **1** + CO<sub>2</sub>, and **1**) in the solid state (KBr disk) at room temperature. (b) HR-ESI-MS spectrum of **1** + CO<sub>2</sub>. The inset exhibits the measured and simulated isotopic patterns at  $m/z$  1188.6480.

spectrum of **1** + CO<sub>2</sub> (Figure 4b) exhibited only a single intense peak at  $m/z$  1188.6480, which could be assigned to the  $[La_4L_4(CO_3)]^{2+}$  cation according to the exact comparison of the intense peak with the simulation based on natural isotopic abundances. This also indicated that transformation of the configuration from circular helicate to quadruple-stranded helicate was achieved by adding CO<sub>2</sub>.

## CONCLUSION

KOH is necessary in the self-assembly process of complexes **4a** and **4b** because it not only deprotonates the ligands as the strong base but also controls the formation of heterotetrametallic triple-stranded helicate assemblies by the  $K^+$  template, and therefore these helicates present high affinity for  $K^+$  and good selectivity over other alkali- and alkaline-earth-metal ions. Conversely, LiOH or NaOH in the self-assembly reactions of complexes **5a** and **5b** appear to only deprotonate the ligands, while CO<sub>2</sub> is responsible for the selection of different structures.

In conclusion, the ligand H<sub>2</sub>L design is versatile enough to initiate and direct different multiple helical supermolecular clusters under different templates to realize the recognition of different ions and molecules (Figure 5). Consequently, the first s–f heterotetrametallic triple-stranded helicate clusters and tetranuclear quadruple-stranded lanthanide helicate clusters fixing CO<sub>2</sub> effectively were assembled. These first examples of lanthanide helicate clusters, as opposed to crown or lariat ether compounds, have two cuplike cavities with oxygen-donor atoms located at two ends for selective  $K^+$  recognition, exhibiting high selectivity over other alkali and alkaline-earth ions. Under the same alkaline conditions but without

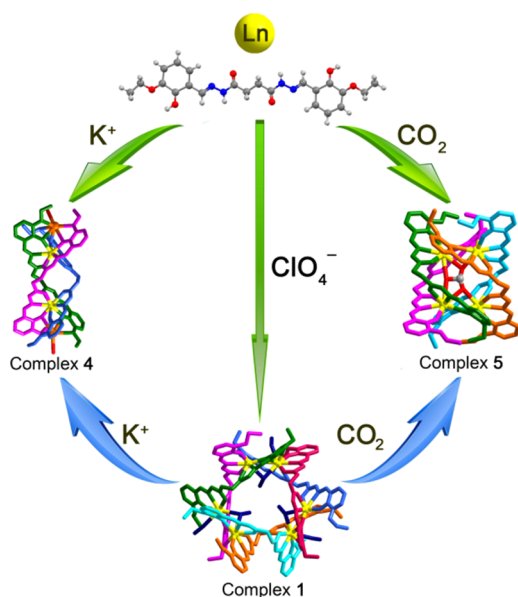


**Figure 5.** Schematic representation of the multiplex self-assembly and reconfiguration of lanthanide helicate clusters induced by ions and molecules (La, yellow; K, orange; N, blue; O, red; C, gray). The ligands are represented by different colors. Hydrogen atoms, external counteranions, and solvent molecules are hidden for clarity.

potassium, new tetranuclear quadruple-stranded helicate lanthanide complexes were fabricated by atmospheric  $\text{CO}_2$ -induced supramolecular self-assembly. On the other hand, these intelligent supermolecular transformers can also be transformed by different external stimuli and, in this process, realize the selective recognition and fixation of the corresponding ions and molecules.  $\text{K}^+$  successfully induced transformation of the configuration from circular helicate to heterotetrametallic triple-stranded helicate, and  $\text{CO}_2$  successfully induced reconfiguration from circular helicate to tetranuclear quadruple-stranded helicate. DNA and proteins often change their helical structure in response to particular external stimuli and can activate important related events through sophisticated mechanisms, and our intelligent supermolecular transformers have successfully simulated this feature.

## EXPERIMENTAL METHODS

**General Procedures.** 3-Methoxysalicylaldehyde and 3-ethoxysalicylaldehyde were purchased from Alfa Aesar and used without further purification. All solvents and other reagents were of reagent-grade quality. Elemental analyses were tested by an Elementar Vario El instrument. HR-ESI-MS was performed on the Fourier transform ion cyclotron resonance mass spectrometers Bruker Apex IV FTMS and Agilent 6210 ESI/TOF. IR spectra were recorded on a Nicolet Avatar 360 FT-IR instrument.  $^1\text{H}$  NMR (400 MHz) and  $^1\text{H}$  NMR (600 MHz) were recorded on a JEOL JNM-ECS 400 M NMR spectrometer and a Varian Mercury Plus 400, respectively. Solid-state  $^{13}\text{C}$  NMR spectra were performed on a Bruker AV400 spectrometer.

**Synthesis of Ligands.** The synthesis routes of our ligands  $\text{H}_2\text{L}'$  and  $\text{H}_2\text{L}$  are simple and easy, which followed our published procedure (shown in Scheme 1).<sup>12</sup>

**Synthesis of Complex 3.** A total of 2 mL of methanol containing 0.1 mmol of  $\text{CeCl}_3 \cdot 7\text{H}_2\text{O}$  (37.3 mg) was added in batches to a stirred solution of 5 mL of *N,N*-dimethylformamide (DMF) of 0.1 mmol of  $\text{H}_2\text{L}'$  (41.4 mg). The mixture was stirred in air for 4 h at room temperature, and then a black solution was formed. The solution was filtered and then exposed to air. Black block single crystals of  $\text{Ce}_2\text{L}'_3$ , which are suitable for X-ray crystallography, were obtained upon slow

evaporation over 1 month (Figure S3). Elem. anal. Calcd for 3 ( $\text{C}_{60}\text{H}_{60}\text{Ce}_2\text{Cl}_2\text{N}_{12}\text{O}_{18}$ ; noncoordinated solvent molecules were lost upon drying): C, 45.39; H, 3.78; N, 10.59. Found: C, 45.40; H, 3.75; N, 10.58. HR-ESI-MS. Found:  $m/z$  758.1103 ( $[\text{Ce}_2\text{L}'_3]^{2+}$ ). Calcd for  $\text{C}_{60}\text{H}_{60}\text{N}_{12}\text{O}_{18}\text{Ce}_2$ :  $m/z$  758.1129 (Figure S4). FT-IR (KBr pellet,  $\text{cm}^{-1}$ ): 3440.0(br), 1600.0(vs), 1557.5(m), 1442.9(s), 1396.0(m), 1365.5(w), 1292.7(s), 1248.4(s), 1073.3(w), 854.9(w), 739.9(m), 567.3(w) (Figure S5).

**Synthesis of Complexes 4a and 4b.** A solution of 0.1 mmol of rare earth halide salt in 2 mL of methanol was added to a light-yellow and transparent solution of  $\text{H}_2\text{L}$  (44.2 mg, 0.1 mmol) with KOH (5.6 mg, 0.2 mmol) after mixing in 8 mL of methanol along with 0.5 mL of DMF. Tetranuclear dimetallic triple-stranded helicates  $[\text{K}_2\text{La}_2\text{L}_3(\text{H}_2\text{O})_2]\text{Br}_2$  (4a; Figure S6) and  $[\text{K}_2\text{Nd}_2\text{L}_3(\text{DMF})_2]\text{Cl}_2$  (4b; Figure S8) were formed by evaporation in air at room temperature over 4 weeks (yield: 50%). Elem. anal. Calcd for 4a ( $\text{C}_{66}\text{H}_{76}\text{Br}_2\text{K}_2\text{La}_2\text{N}_{12}\text{O}_{20}$ ; noncoordinated solvent molecules were lost upon evaporation): C, 42.28; H, 4.06; N, 8.97. Found: C, 42.31; H, 4.01; N, 8.88. HR-ESI-MS. Found:  $m/z$  856.1344 ( $[\text{K}_2\text{La}_2\text{L}_3(\text{H}_2\text{O})_2]^{2+}$ ). Calcd for  $[\text{C}_{66}\text{H}_{72}\text{K}_2\text{La}_2\text{N}_{12}\text{O}_{18}]^{2+}$ :  $m/z$  856.1350 (Figure S10). Elem. anal. Calcd for 4b ( $\text{C}_{72}\text{H}_{86}\text{Cl}_2\text{K}_2\text{Nd}_2\text{N}_{14}\text{O}_{20}$ ; noncoordinated solvent molecules were lost upon drying): C, 45.47; H, 4.53; N, 10.31. Found: C, 45.31; H, 4.41; N, 10.28. HR-ESI-MS. Found:  $m/z$  843.1322 ( $[\text{K}_2\text{Nd}_2\text{L}_3]^{2+}$ ). Calcd for  $[\text{C}_{66}\text{H}_{72}\text{K}_2\text{Nd}_2\text{N}_{12}\text{O}_{18}]^{2+}$ :  $m/z$  843.1285 (Figure S11). FT-IR for 4a and 4b (KBr pellet,  $\text{cm}^{-1}$ ): 3428.11(br), 2958.88(br), 1603.67(vs), 1453.10(s), 1395.30(m), 1365.64(m), 1310.15(m), 1220.38(s), 1175.51(w), 1068.28(m), 1017.33(w), 972.46(w), 888.05(w), 850.5(w), 741.27(s), 656.86(w), 566.36(w) (Figure S9).

**Synthesis of Complexes 5a and 5b.** A total of 0.2 mmol of  $\text{LiOH} \cdot \text{H}_2\text{O}$  or 0.2 mmol of NaOH and 0.1 mmol of  $\text{H}_2\text{L}$  (44.2 mg) were added into a mixing solvent containing 8 mL of methanol and 0.5 mL of DMF, and then the solution was stirred for 10 min. After that, a solution of 0.1 mmol of  $\text{LnCl}_3 \cdot 6\text{H}_2\text{O}$  in 2 mL of methanol was added. The mixture was rapidly stirred for 10 min. Then the solution was filtered and exposed to air. Rhombohedral crystals of  $[\text{La}_4\text{L}_4(\text{CO}_3)]\text{Cl}_2$  (5a; Figure S18) and  $[\text{Nd}_4\text{L}_4(\text{CO}_3)]\text{Cl}_2$  (5b; Figure S20) suitable for X-ray analysis were obtained by slow evaporation over several weeks at room temperature in air (yield: 60%).  $\text{CO}_2$  molecules from air are efficiently captured and fixed by these clusters. Elem. anal. Calcd for 5a ( $\text{C}_{89}\text{H}_{96}\text{Cl}_2\text{La}_4\text{N}_{16}\text{O}_{27}$ ; noncoordinated solvent molecules were lost upon drying): C, 44.94; H, 4.04; N, 9.43. Found: C, 44.71; H, 4.01; N, 9.21. HR-ESI-MS for 5a. Found:  $m/z$  1188.14244 ( $[\text{La}_4\text{L}_4(\text{CO}_3)]^{2+}$ ). Calcd for  $[\text{C}_{89}\text{H}_{96}\text{La}_4\text{N}_{16}\text{O}_{27}]^{2+}$ :  $m/z$  1188.14369 (Figure S21). Elem. anal. Calcd for 5b ( $\text{C}_{89}\text{H}_{96}\text{Cl}_2\text{Nd}_4\text{N}_{16}\text{O}_{27}$ ; noncoordinated solvent molecules were lost upon drying): C, 43.34; H, 3.90; N, 9.09. Found: C, 43.61; H, 3.98; N, 9.13. HR-ESI-MS. Found:  $m/z$  1197.1517 ( $[\text{Nd}_4\text{L}_4(\text{CO}_3)]^{2+}$ ). Calcd for  $[\text{C}_{89}\text{H}_{96}\text{Nd}_4\text{N}_{16}\text{O}_{27}]^{2+}$ :  $m/z$  1197.1509 (Figure S22). FT-IR for 5a and 5b (KBr pellet,  $\text{cm}^{-1}$ ): 3402.00(br), 3180.44(br), 2974.75(br), 1642.97(vs), 1610.00(vs), 1552.44(m), 1500.00(w), 1450.00(s), 1392.02(m), 1308.63(w), 1218.10(s), 1070.39(m), 973.50(w), 883.77(w), 844.85(w), 742.40(w), 651.87(w), 562.13(w) (Figure S25).

**Caution!** There were no problems involved during the preparation of rare earth halide salts and hydrazine hydrate, but suitable care should be taken when handling such potentially hazardous compounds.

## ASSOCIATED CONTENT

### Supporting Information

The Supporting Information is available free of charge at <https://pubs.acs.org/doi/10.1021/acs.inorgchem.0c03617>.

Synthetic details and characterization, binding constant, and kinetic experiments (PDF)

### Accession Codes

CCDC 1470814–1470816, 1470818, and 1817349 contain the supplementary crystallographic data for this paper. These data can be obtained free of charge via [www.ccdc.cam.ac.uk/](http://www.ccdc.cam.ac.uk/)

data\_request/cif, or by emailing [data\\_request@ccdc.cam.ac.uk](mailto:data_request@ccdc.cam.ac.uk), or by contacting The Cambridge Crystallographic Data Centre, 12 Union Road, Cambridge CB2 1EZ, UK; fax: +44 1223 336033.

## AUTHOR INFORMATION

### Corresponding Authors

**Bei Wang** – Key Laboratory of Nonferrous Metals Chemistry and Resources Utilization of Gansu Province, State Key Laboratory of Applied Organic Chemistry, and College of Chemistry and Chemical Engineering, Lanzhou University, Lanzhou 730000, China; [orcid.org/0000-0002-3898-6974](https://orcid.org/0000-0002-3898-6974); Email: [wangbei@lzu.edu.cn](mailto:wangbei@lzu.edu.cn)

**Weisheng Liu** – Key Laboratory of Nonferrous Metals Chemistry and Resources Utilization of Gansu Province, State Key Laboratory of Applied Organic Chemistry, and College of Chemistry and Chemical Engineering, Lanzhou University, Lanzhou 730000, China; [orcid.org/0000-0001-5448-6315](https://orcid.org/0000-0001-5448-6315); Email: [liuwens@lzu.edu.cn](mailto:liuwens@lzu.edu.cn)

### Authors

**Bing Ma** – Department of Orthopedics, Lanzhou University Second Hospital, Lanzhou 730000, China

**Zhangwen Wei** – MOE Laboratory of Bioinorganic and Synthetic Chemistry/KLGHEI of Environment and Energy Chemistry, Lehn Institute of Functional Materials, School of Chemistry and Chemical Engineering, Sun Yat-Sen University, Guangzhou 510275, China

**Huan Yang** – Key Laboratory of Nonferrous Metals Chemistry and Resources Utilization of Gansu Province, State Key Laboratory of Applied Organic Chemistry, and College of Chemistry and Chemical Engineering, Lanzhou University, Lanzhou 730000, China

**Meng Wang** – Biochemistry Teaching and Research Section, Gangou Middle School of Jingning, Pingliang 743400, China

**Wenxia Yin** – Biochemistry Teaching and Research Section, Gangou Middle School of Jingning, Pingliang 743400, China

**Hong Gao** – Key Laboratory of Nonferrous Metals Chemistry and Resources Utilization of Gansu Province, State Key Laboratory of Applied Organic Chemistry, and College of Chemistry and Chemical Engineering, Lanzhou University, Lanzhou 730000, China

Complete contact information is available at:  
<https://pubs.acs.org/10.1021/acs.inorgchem.0c03617>

### Author Contributions

<sup>†</sup>These authors contributed equally.

### Notes

The authors declare no competing financial interest.

## ACKNOWLEDGMENTS

The authors acknowledge the National Natural Science Foundation of China (Projects 21401090, 21431002, 21871122, and 21707059).

## REFERENCES

(1) (a) Stomeo, F.; Lincheneau, C.; Leonard, J. P.; O'Brien, J. E.; Peacock, R. D.; McCoy, C. P.; Gunnlaugsson, T. Metal-Directed Synthesis of Enantiomerically Pure Dimetallic Lanthanide Luminescent Triple-Stranded Helicates. *J. Am. Chem. Soc.* **2009**, *131*, 9636–9637. (b) Zebret, S.; Vögele, E.; Klumpler, T.; Hamacek, J. Designing Artificial 3D Helicates: Unprecedented Self-Assembly of Homooctanuclear Tetrapods with Europium. *Chem. - Eur. J.* **2015**, *21*,

6695–6699. (c) Barry, D. E.; Caffrey, D. F.; Gunnlaugsson, T. Lanthanide-directed synthesis of luminescent self-assembly supramolecular structures and mechanically bonded systems from acyclic coordinating organic ligands. *Chem. Soc. Rev.* **2016**, *45*, 3244–3274. (d) Yeung, C.-T.; Chan, W. T. K.; Yan, S.-C.; Yu, K.-L.; Yim, K.-H.; Wong, W.-T.; Law, G.-L. Lanthanide Supramolecular Helical Diastereoselective Breaking Induced by Point Chirality: Mixture or P-helix, M-helix. *Chem. Commun.* **2015**, *51*, 592–595. (e) Habib, F.; Long, J.; Lin, P.-H.; Korobkov, I.; Ungur, L.; Wernsdorfer, W.; Chibotaru, L. F.; Murugesu, M. Supramolecular Architectures for Controlling Slow Magnetic Relaxation in Field-Induced Single-Molecule Magnets. *Chem. Sci.* **2012**, *3*, 2158–2164. (f) Terazzi, E.; Guénee, L.; Varin, J.; Bocquet, B.; Lemonnier, J.-F.; Emery, D.; Mareda, J.; Piguet, C. Silver Baits for The “Miraculous Draught” of Amphiphilic Lanthanide Helicates. *Chem. - Eur. J.* **2011**, *17*, 184–195. (g) Xing, P.; Zhao, Y. Controlling Supramolecular Chirality in Multicomponent Self-Assembled Systems. *Acc. Chem. Res.* **2018**, *51*, 2324–2334. (h) Li, H.; Yao, Z.-J.; Liu, D.; Jin, G.-X. Multi-component coordination-driven self-assembly toward heterometallic macrocycles and cages. *Coord. Chem. Rev.* **2015**, *293–294*, 139–157. (2) (a) dos Santos, C. M. G.; Harte, A. J.; Quinn, S. J.; Gunnlaugsson, T. Recent Developments in the Field of Supramolecular Lanthanide Luminescent Sensors and Self-Assemblies. *Coord. Chem. Rev.* **2008**, *252*, 2512–2527. (b) Bünzli, J.-C. G.; Piguet, C. Taking Advantage of Luminescent Lanthanide Ions. *Chem. Soc. Rev.* **2005**, *34*, 1048–1077. (c) Montgomery, C. P.; Murray, B. S.; New, E. J.; Pal, R.; Parker, D. Cell-Penetrating Metal Complex Optical Probes: Targeted and Responsive Systems Based on Lanthanide Luminescence. *Acc. Chem. Res.* **2009**, *42*, 925–937. (d) Binnemans, K. Lanthanide-Based Luminescent Hybrid Materials. *Chem. Rev.* **2009**, *109*, 4283–4374. (e) Lin, S.-Y.; Zhao, L.; Guo, Y.-N.; Zhang, P.; Guo, Y.; Tang, J. Two New Dy<sub>3</sub> Triangles with Trinuclear Circular Helicates and Their Single-Molecule Magnet Behavior. *Inorg. Chem.* **2012**, *51*, 10522–10528. (f) Sahoo, J.; Arunachalam, R.; Subramanian, P. S.; Suresh, E.; Valkonen, A.; Rissanen, K.; Albrecht, M. Coordinatively Unsaturated Lanthanide(III) Helicates: Luminescence Sensors for Adenosine Monophosphate in Aqueous Media. *Angew. Chem., Int. Ed.* **2016**, *55*, 9625–9629. (3) (a) Aroussi, B. E.; Zebret, S.; Besnard, C.; Perrotet, P.; Hamacek, J. Rational Design of a Ternary Supramolecular System: Self-Assembly of Pentanuclear Lanthanide Helicates. *J. Am. Chem. Soc.* **2011**, *133*, 10764–10767. (b) Chen, W.; Tang, X.; Dou, W.; Wang, B.; Guo, L.; Ju, Z.; Liu, W. The Construction of Homochiral Lanthanide Quadruple-Stranded Helicates with Multiresponsive Sensing Properties toward Fluoride Anions. *Chem. - Eur. J.* **2017**, *23*, 9804–9811. (c) Li, X.; Zhou, L.; Yan, L.; Yuan, D.; Lin, C.; Sun, Q. Evolution of Luminescent Supramolecular Lanthanide M<sub>2n</sub>L<sub>3n</sub> Complexes from Helicates and Tetrahedra to Cubes. *J. Am. Chem. Soc.* **2017**, *139*, 8237–8244. (d) Bing, T. Y.; Kawai, T.; Yuasa, J. Ligand-to-Ligand Interactions That Direct Formation of D<sub>2</sub>-Symmetrical Alternating Circular Helicate. *J. Am. Chem. Soc.* **2018**, *140*, 3683–3689. (e) Zare, D.; Suffren, Y.; Nozary, H.; Hauser, A.; Piguet, C. Controlling Lanthanide Exchange in Triple-Stranded Helicates: A Way to Optimize Molecular Light-Upconversion. *Angew. Chem., Int. Ed.* **2017**, *56*, 14612–14617. (4) (a) Ha, S. C.; Lowenhaupt, K.; Rich, A.; Kim, Y.-G.; Kim, K. K. Crystal structure of a junction between B-DNA and Z-DNA reveals two extruded bases. *Nature* **2005**, *437*, 1183–1186. (b) Crespo, L.; Sanclimens, G.; Montaner, B.; Pérez-Tomás, R.; Royo, M.; Pons, M.; Albericio, F.; Giralt, E. Peptide Dendrimers Based on Polyproline Helices. *J. Am. Chem. Soc.* **2002**, *124*, 8876–8883. (c) Xu, M.; Liu, L.; Yan, Q. Allosterically Activated Protein Self-Assembly for the Construction of Helical Microfilaments with Tunable Helicity. *Angew. Chem., Int. Ed.* **2018**, *57*, 5029–5032. (d) Bisoyi, H. K.; Bunning, T. J.; Li, Q. Stimuli-Driven Control of the Helical Axis of Self-Organized Soft Helical Superstructures. *Adv. Mater.* **2018**, *30*, 1706512–1706547. (5) Wu, W.; Kirillov, A. M.; Yan, X.; Zhou, P.; Liu, W.; Tang, Y. Enhanced Separation of Potassium Ions by Spontaneous K<sup>+</sup>-Induced

Self-Assembly of a Novel Metal-Organic Framework and Excess Specific Cation- $\pi$  Interactions. *Angew. Chem., Int. Ed.* **2014**, *53*, 10649–10653.

(6) (a) Liu, Z.; Luo, F.; Ju, X.-J.; Xie, R.; Luo, T.; Sun, Y.-M.; Chu, L.-Y. Positively  $K^+$ -Responsive Membranes with Functional Gates Driven by Host-Guest Molecular Recognition. *Adv. Funct. Mater.* **2012**, *22*, 4742–4750. (b) He, X.; Yam, V. W.-W. A Highly Selective Bifunctional Luminescence Probe for Potassium and Fluoride Ions. *Org. Lett.* **2011**, *13*, 2172–2175. (c) Wei, W.; Xu, C.; Ren, J.; Xu, B.; Qu, X. Sensing metal ions with ion selectivity of a crown ether and fluorescence resonance energy transfer between carbon dots and graphene. *Chem. Commun.* **2012**, *48*, 1284–1286. (d) Qin, H.; Ren, J.; Wang, J.; Luedtke, N. W.; Wang, E. G-Quadruplex-Modulated Fluorescence Detection of Potassium in the Presence of a 3500-Fold Excess of Sodium Ions. *Anal. Chem.* **2010**, *82*, 8356–8360. (e) Vantomme, G.; Lehn, J.-M. Photo- and Thermoresponsive Supramolecular Assemblies: Reversible Photorelease of  $K^+$  Ions and Constitutional Dynamics. *Angew. Chem., Int. Ed.* **2013**, *52*, 3940–3943.

(7) (a) Xu, J.; Raymond, K. N. Structurally Characterized Quadruple-Stranded Bisbidentate Helicates. *Angew. Chem., Int. Ed.* **2006**, *45*, 6480–6485. (b) Zhu, X.; He, C.; Dong, D.; Liu, Y.; Duan, C. Cerium-Based Triple-Stranded Helicates as Luminescent Chemosensors for the Selective Sensing of Magnesium Ions. *Dalton Trans.* **2010**, *39*, 10051–10055. (c) Chen, W.; Tang, X.; Dou, W.; Ju, Z.; Xu, B.; Xu, W.; Liu, W.  $K^+$ -Induced in situ self-assembly of near-infrared luminescent membrane material armored with bigger Yb(III) complex crystallites. *Chem. Commun.* **2016**, *52*, 5124–5127. (d) Albrecht, M.; Osetka, O.; Fröhlich, R.; Bünzli, J.-C. G.; Aebischer, A.; Gumy, F.; Hamacek, J. Highly Efficient Near-IR Emitting Yb/Yb and Yb/Al Helicates. *J. Am. Chem. Soc.* **2007**, *129*, 14178–14179.

(8) (a) Thibon, A.; Pierre, V. C. A Highly Selective Luminescent Sensor for the Time-Gated Detection of Potassium. *J. Am. Chem. Soc.* **2009**, *131*, 434–435. (b) Weitz, E. A.; Pierre, V. C. A Ratiometric Probe for the Selective Time-Gated Luminescence Detection of Potassium in Water. *Chem. Commun.* **2011**, *47*, 541–543. (c) Junker, A. K. R.; Tropiano, M.; Faulkner, S.; Sørensen, T. J. Kinetically Inert Lanthanide Complexes as Reporter Groups for Binding of Potassium by 18-crown-6. *Inorg. Chem.* **2016**, *55*, 12299–12308.

(9) (a) Olah, G. A.; Goepfert, A.; Prakash, G. K. S. Chemical Recycling of Carbon Dioxide to Methanol and Dimethyl Ether: From Greenhouse Gas to Renewable, Environmentally Carbon Neutral Fuels and Synthetic Hydrocarbons. *J. Org. Chem.* **2009**, *74*, 487–498. (b) Caldeira, K.; Jain, A. K.; Hoffert, M. I. Climate sensitivity uncertainty and the need for energy without  $CO_2$  emission. *Science* **2003**, *299*, 2052–2054. (c) Toda, Y.; Komiyama, Y.; Kikuchi, A.; Suga, H. Tetraarylphosphonium Salt-Catalyzed Carbon Dioxide Fixation at Atmospheric Pressure for the Synthesis of Cyclic Carbonates. *ACS Catal.* **2016**, *6*, 6906–6910. (d) Seo, U. R.; Chung, Y. K. Potassium phosphate-catalyzed one-pot synthesis of 3-aryl-2-oxazolidinones from epoxides, amines, and atmospheric carbon dioxide. *Green Chem.* **2017**, *19*, 803–808.

(10) Representative references: (a) Olah, G. A. Beyond Oil and Gas: The Methanol Economy. *Angew. Chem., Int. Ed.* **2005**, *44*, 2636–2639. (b) Kong, L. Y.; Zhang, Z. H.; Zhu, H. F.; Kawaguchi, H.; Okamura, T.; Doi, M.; Chu, Q.; Sun, W. Y.; Ueyama, N. Copper (II) and Zinc (II) Complexes can Fix Atmospheric Carbon Dioxide. *Angew. Chem., Int. Ed.* **2005**, *44*, 4352–4355. (c) García-España, E.; Gaviña, P.; Latorre, J.; Soriano, C.; Verdejo, B.  $CO_2$  Fixation by Copper (II) Complexes of a Terpyridinophane Aza Receptor. *J. Am. Chem. Soc.* **2004**, *126*, 5082–5083. (d) Gao, G.; Wang, L.; Zhang, R.; Xu, C.; Yang, H.; Liu, W. S. Hexanuclear 3d-4f complexes as efficient catalysts for converting  $CO_2$  into cyclic carbonates. *Dalton Trans.* **2019**, *48*, 3941–3945.

(11) (a) Tang, X. L.; Wang, W. H.; Dou, W.; Jiang, J.; Liu, W. S.; Qin, W. W.; Zhang, G. L.; Zhang, H. R.; Yu, K. B.; Zheng, L. M. Olive-Shaped Chiral Supramolecules: Simultaneous Self-Assembly of Heptameric Lanthanum Clusters and Carbon Dioxide Fixation. *Angew. Chem., Int. Ed.* **2009**, *48*, 3499–3502. (b) Yang, H.; Gao,

G.; Chen, W.; Wang, L.; Liu, W. S. Self-assembly of tetranuclear 3d-4f helicates as highly efficient catalysts for  $CO_2$  cycloaddition reactions under mild conditions. *Dalton Trans.* **2020**, *49*, 10270–10277. (c) Wang, L.; Xu, C.; Han, Q. X.; Tang, X. L.; Zhou, P. P.; Zhang, R. L.; Gao, G. S.; Xu, B. H.; Qin, W. W.; Liu, W. S. Ambient chemical fixation of  $CO_2$  using a highly efficient heterometallic helicate catalyst system. *Chem. Commun.* **2018**, *54*, 2212–2215. (d) Wang, L.; Zhang, R.; Han, Q.; Xu, C.; Chen, W.; Yang, H.; Gao, G.; Qin, W.; Liu, W. S. Amide-functionalized heterometallic helicate cages as highly efficient catalysts for  $CO_2$  conversion under mild conditions. *Green Chem.* **2018**, *20*, 5311–5317.

(12) Wang, B.; Zang, Z.; Wang, H.; Dou, W.; Tang, X.; Liu, W.; Shao, Y.; Ma, J.; Li, Y.; Zhou, J. Multiple Lanthanide Helicate Clusters and the Effects of Anions on Their Configuration. *Angew. Chem., Int. Ed.* **2013**, *52*, 3756–3759.

(13) (a) Swamy, S. I.; Bacsa, J.; Jones, J. T. A.; Stylianou, K. C.; Steiner, A.; Ritchie, L. K.; Hasell, T.; Gould, J. A.; Laybourn, A.; Khimyak, Y. Z.; Adams, D. J.; Rosseinsky, M. J.; Cooper, A. I. A Metal-Organic Framework with a Covalently Prefabricated Porous Organic Linker. *J. Am. Chem. Soc.* **2010**, *132*, 12773–12775. (b) Rivas, M.; del Valle, L. J.; Turon, P.; Alemán, C.; Puiggali, J. Sustainable synthesis of amino acids by catalytic fixation of molecular dinitrogen and carbon dioxide. *Green Chem.* **2018**, *20*, 685–693.

(14) (a) Langley, S. K.; Moubaraki, B.; Murray, K. S. Magnetic Properties of Hexanuclear Lanthanide(III) Clusters Incorporating a Central  $\mu_6$ -Carbonate Ligand Derived from Atmospheric  $CO_2$  Fixation. *Inorg. Chem.* **2012**, *51*, 3947–3949. (b) Guo, Y. N.; Chen, X. H.; Xue, S.; Tang, J. Molecular Assembly and Magnetic Dynamics of Two Novel  $Dy_6$  and  $Dy_8$  Aggregates. *Inorg. Chem.* **2012**, *51*, 4035–4042.